

Persistence of iron(II) in surface waters of the western subarctic Pacific

Eric G. Roy¹ and Mark L. Wells

School of Marine Sciences, University of Maine, Orono, Maine 04469

D. Whitney King

Department of Chemistry, Colby College, Waterville, Maine 04901

Abstract

The distribution of dissolved iron(II) [Fe(II)] was studied in surface waters of the western subarctic Pacific during the Subarctic Pacific Iron Experiment for Ecosystem Dynamics Study-II (SEEDS II) iron enrichment experiment using highly sensitive flow injection-based luminol chemiluminescence. Vertical profiles of Fe(II) and total dissolved iron were measured outside of the fertilized patch to investigate the chemical speciation of iron in this high-nitrate low-chlorophyll (HNLC) region. Ambient total dissolved iron concentrations ranged from 50 pmol L⁻¹ to 150 pmol L⁻¹ depending on depth and sampling times. Unexpectedly, Fe(II) accounted for up to half of total dissolved iron, with concentrations up to ~50 pmol L⁻¹. Fe(II) concentrations decreased exponentially with depth and were undetectable at depths below 50 m. There was no evidence of increased Fe(II) concentrations associated with the subsurface chlorophyll maximum, indicating that photolysis, rather than biological reduction of Fe(III), was the primary source of Fe(II). Because Fe(II) concentrations in the fertilized patch remained elevated for more than a week after enrichment, Fe(II) oxidation rates at near-ambient concentrations were measured. Indeed, the temperature-dependent Fe(II) oxidation rates were significantly slower than predicted by Fe(II) oxidation models and rates measured in ligand-free seawater. These findings suggest that Fe(II) binding ligands may exist in these HNLC waters, with conditional stability constants on the order of 10⁸–10⁹ with respect to Fe²⁺. The accumulation of Fe(II) during daylight hours did not alleviate iron limitation of eukaryotic phytoplankton in these waters, contrary to expectations from recent iron uptake models.

The constraint of carbon export by iron (Fe) supply in the high-nitrate low-chlorophyll (HNLC) regions of the Southern Ocean, equatorial Pacific, and subarctic Pacific is now well demonstrated, but the inability of diatoms and other eukaryotic phytoplankton to fully utilize the ambient iron pools in these waters is much less understood. The thresholds for diffusion-limited iron uptake, for even large pennate diatoms, are <10 pmol L⁻¹ (Hudson and Morel 1993; Wells 2003), yet dissolved iron concentrations in HNLC regions are often an order of magnitude higher. The overwhelming (~99%) control of iron speciation by high-affinity organic chelators (*see* Rue and Bruland 1997) is believed to restrict iron availability to diatoms, however, this expectation stems from the assumption that iron speciation is at or near equilibrium in surface ocean waters. At equilibrium, inorganic iron concentrations are <0.1 pmol L⁻¹ (Rue and Bruland 1997), a level too low to support the growth of large oceanic phytoplankton (Brand et al. 1983; Sunda and Huntsman 1995; Wells 2003), and thermochemical dissociation rates of these complexes are too slow to replenish the inorganic Fe(III) species sequestered by uptake (Hudson and Morel 1993; Wells and Trick 2004). The apparently ubiquitous excess of these

strong iron-specific organic ligands in HNLC waters (Rue and Bruland 1997) challenges the current view that natural iron deposition events can transform phytoplankton communities, because even large aerosol inputs to the ocean cause only subnanomolar increases of dissolved iron in surface waters (Sedwick et al. unpubl.).

Photochemical cycling of Fe(III) is known to occur in surface ocean waters (Kuma et al. 1992; Johnson et al. 2004; Miller et al. 1995), and the photochemical action spectrum for these transformations suggests they can occur deep into the photic zone (Wells et al. 1991; Laglera and Van Den Berg 2007). Despite this, the net effect of photolysis on iron speciation generally has been assumed to be small because of rapid reoxidation of photoproduct Fe(II) in oxic seawater (King et al. 1995). Kinetic models have suggested that steady-state inorganic iron [Fe(III) plus Fe(II)] concentrations increase to only a few percent of total dissolved iron under full sunlight (Sunda and Huntsman 1995; Rue and Bruland 1997). This expectation has been challenged recently, particularly in cold seawaters where Fe(II) oxidation kinetics are substantially slower (Croot et al. 2001). Moreover, the apparent use of reductive, high-affinity iron uptake systems by some diatoms (Maldonado and Price 2001; Wells et al. 2005) suggests that photoproduct Fe(II) may be readily accessible. However, the extent that these redox processes change iron speciation in natural seawater is not well understood.

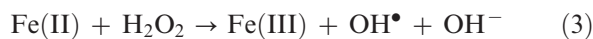
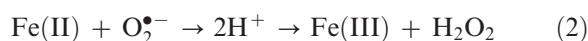
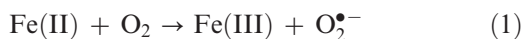
Fe(II) oxidation in natural waters is controlled largely by reactions with dissolved oxygen and hydrogen peroxide. In most open ocean surface waters, hydrogen peroxide concentrations are significantly below 200 nmol L⁻¹

¹ Corresponding author (eric.roy@umit.maine.edu).

Acknowledgments

We thank the captain and crew of the R/V *Kilo Moana*. The authors also thank two anonymous reviewers for their helpful comments on this work. This work was funded by NSF Grants OCE-0241752 and BES-0304523, and additional student support was provided by NSF GK-12 (DGE-0231642) and IGERT Sensors (0504494) Fellowships.

(O'sullivan et al. 2005), and Fe(II) oxidation is dominated by dissolved oxygen (Santana-Casiano et al. 2006). The Haber–Weiss mechanism is the most widely accepted process used to describe Fe(II) oxidation in oxic seawater, with Reactions 1 or 3 limiting the overall oxidation rate (King et al. 1995).



The rates for Eqs. 1–4 are highly dependant on the relative concentrations of the individual Fe(II) species in solution (Millero 1989; King 1998; Santana-Casiano et al. 2006). A solution of hydrated Fe^{2+} has an oxidative half-life on the order of days to weeks, but trace amounts of highly-reactive Fe(OH)_2^0 can reduce the overall half-life to a few seconds (King 1998). Temperature is another parameter that controls overall Fe(II) oxidation rates in seawater. The half-life of Fe(II) is expected to be a few minutes in warm (tropical, subtropical) seawater, but can extend to an hour or more in cold polar waters (Croot et al. 2001).

There is evidence that Fe(II) can constitute a significant, though small, fraction of dissolved iron in natural seawater (*see* Rose and Waite 2002). But are these observations due only to temperature effects, or is there a kinetically less reactive species that slows oxidation enough to enable significant concentrations of Fe(II) to accumulate? Organic Fe(II) complexing ligands are known to slow Fe(II) oxidation rates in freshwater systems, and there is evidence that they also exist in rainwater (*see* Kieber et al. 2005), but their presence in seawater remains speculative. Even modest buffering of inorganic Fe(II) concentrations during daylight hours might have substantial implications for eukaryotic phytoplankton that use reductive uptake mechanisms for iron acquisition (Shaked et al. 2005; Wells et al. 2005; Salmon et al. 2006).

In this work, we used flow injection-based luminol chemiluminescence to measure Fe(II) in surface waters of the iron-limited subarctic Pacific. We show that Fe(II) concentrations in near-surface waters are consistent with a photochemical (rather than a biological) source and that Fe(II) can account for a significant fraction of the total dissolved iron in these waters. Fe(II) oxidation rates were measured in surface HNLC waters across a range of temperatures (4.0–21.0°C) at near-ambient Fe(II) concentrations ($[\text{Fe(II)}]_0 = 0.1 \text{ nmol L}^{-1}$). Additionally, low-level Fe(II) oxidation rates were measured in ligand-free seawater for the same range of temperatures. Although analytically challenging, these experimental conditions minimized the contributions of Eqs. 2–4 to overall Fe(II) oxidation rates and will greatly simplify comparisons to current oxidation models and future work. Our results show that Fe(II) oxidation rates in these surface seawaters are substantially slower than rates measured in ligand-free

seawater, providing indirect evidence that Fe(II) complexing ligands can control iron speciation and thereby its availability to phytoplankton in surface waters of the western subarctic Pacific.

Materials and methods

Sampling—Samples were collected during the SEEDS II mesoscale iron enrichment experiment in July and August 2004 from both within (in patch) and outside (out patch) the fertilized patch near 46.7°N, 165.8°E. Underway samples were drawn through 1-cm internal diameter Teflon polytetrafluoroethylene (PFA) tubing from the nose of an all-plastic towfish and pumped on board with a Teflon double diaphragm pump. The towfish was positioned 8 m outboard of the hull using the boom of the ship so it lay outside the wash of the ship. The tubing was shielded from sunlight to minimize photochemical effects during sample collection, either by the Kevlar reinforcing sheath of the tow segment or by black plastic on deck. The sampling station for pumped water was situated under a High Efficiency Particulate Air Filter (HEPA) bench inside a positive-pressure shipboard cleanroom. Deep-water samples were collected from X-Niskin bottles deployed on a Kevlar line, triggered by a Teflon messenger. To shorten the time between sample collection and analysis, the X-Niskin bottles were gravity filtered (0.2 μm) while still on the Kevlar line, using a protective bell to minimize sample contamination. Both towfish and bottle sampling techniques delivered seawater to the analysis area quickly enough (<45 s) that Fe(II) measurements did not require correction for oxidative losses between sampling and analysis (*see* below).

Samples for total iron analysis were filtered through a 0.2- μm capsule filter (pumped surface water, PCI Membrane Systems; vertical profile, Millipore) at low pressure (<70 kPa) and collected in rigorously cleaned Teflon bottles. Samples for Fe(II) analyses were filtered and collected in darkened (external tape) 125-mL Teflon bottles. The flow injection system was positioned in a separate cleanroom directly adjacent to the towfish sampling station and was contained in a HEPA bench surrounded by black plastic sheeting to limit sample exposure to laboratory fluorescent lighting.

Reagents—All solutions were prepared using >18 M Ω water from a Millipore Milli-Q Gradient A10 TOC purification system. All chemicals were of the highest commercially available purity and were used as received: luminol [5-amino-2,3-(dihydroxymethyl)aminomethane] (Fluka); ferrous ammonium sulfate hexahydrate, ferric iron standard, potassium carbonate, and sodium sulfite (Sigma); and concentrated hydrochloric acid (HCl), ammonia, and glacial acetic acid (Optima, Fisher). The luminol reagent was prepared according to King et al. (1995), except the alkaline luminol reagent pH was set using Optima grade ammonia. Cold (8.0°C) seawater that had been aged in the dark for 24 h was used as a carrier solution. The luminol reagent and carrier solutions were stored in acid-cleaned polyethylene bottles and kept in the dark.

Fe(II) analysis—Fe(II) was analyzed using an automated flow injection-based FeLume system (Waterville Analytical) described in detail by King et al. (1995). Briefly, an alkaline luminol solution reacted with Fe(II) to generate light, according to the reaction mechanism described in detail by others (see Xiao et al. 2002). Labview software (National Instruments) controlled the loading and injection of a 1-m loop of 1.59-mm outside diameter Teflon tubing, and subsequent mixing of sample and luminol solution occurred in a plexiglas reaction spiral set under a photomultiplier tube. During Fe(II) analysis, the sample loops were kept in an ice bath to minimize Fe(II) oxidative loss as the sample flowed to the reaction spiral. The intensity of the burst luminescence was recorded as the sample passed through the reaction coil, and the peak was integrated to quantify the signal. This approach generated intense peaks that enabled highly sensitive Fe(II) determinations at ambient seawater pH without need for sample preconcentration. At the high pH of the chemiluminescence reaction, mineral precipitates slowly coat the inside of the reaction spiral, attenuating the chemiluminescence signal. This problem was avoided by rinsing the reaction spiral with 0.01 mol L⁻¹ HCl between samples.

Instrument optimization was performed daily by continuously pumping a 100 pmol L⁻¹ Fe(II) standard directly into the reaction coil, along with luminol, and adjusting the photomultiplier tube (PMT) and pump parameters to optimize the signal-to-noise ratio. Analytical precision was greatly improved by carefully monitoring tension adjustments on the peristaltic pump to ensure very smooth reagent and carrier flow. The acid-cleaned Viton (Cole Parmer) pump tubing wore slowly, requiring some daily adjustment of sample loading times, and was replaced after 30–50 h of continuous use.

A 0.01 mol L⁻¹ primary Fe(II) stock solution was prepared by dissolving Fe(NH₄)₂(SO₄)₂·6H₂O in 50 mL of 0.1 mol L⁻¹ HCl and was used throughout the cruise. Secondary Fe(II) stock solutions of 10 μmol L⁻¹ and 100 nmol L⁻¹ were prepared 30 min before running the standard curve by diluting the primary stock in 0.001 mol L⁻¹ and 0.0005 mol L⁻¹ HCl, respectively. Individual Fe(II) standards were prepared in dark aged seawater by diluting the secondary stock solutions immediately before analysis. All standards were analyzed in triplicate, whereas analytical blanks had ≥5 replicates. During analysis, all samples and standards were maintained in a temperature-controlled bath (Neslab) at 8.0°C to more closely match ambient surface-water temperatures and to minimize oxidative loss of Fe(II) during analysis. Standards were run from high to low concentration to determine appropriate peak integration limits and to test for carryover between samples. Although the chemiluminescence response to Fe(II) is generally nonlinear across wider concentration ranges, our standard curves were linear over 0–1,500 pmol L⁻¹. The regression slope and intercepts varied from day to day, likely because of the age of the luminol reagent. The Fe(II) analytical detection limits (3 × SD of reagent blank values) ranged from 1 pmol L⁻¹ to 11 pmol L⁻¹, and the blank value was indistinguishable from the instrument baseline because the carrier was Fe(II)-

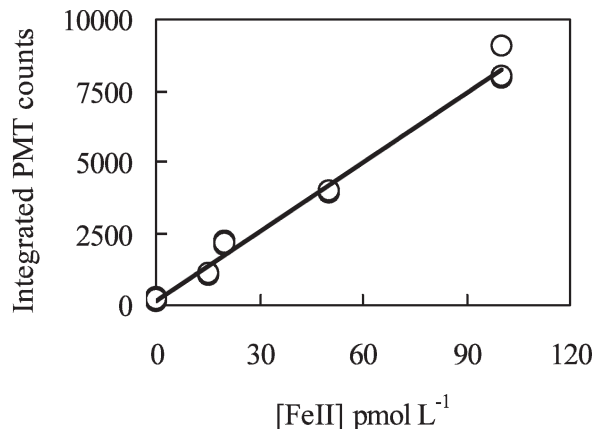


Fig. 1. A representative standard curve for Fe(II) analysis by luminol chemiluminescence. Standards were analyzed in triplicate, with all replicates shown on the plot. The analytical detection limit on this day was 2 pmol L⁻¹ (3 × SD of the reagent blank).

free seawater and Fe(II) is quickly eliminated in the alkaline luminol reagent. A representative Fe(II) standard curve is shown in Fig. 1.

Total Fe analysis—Total iron concentrations were determined by chemically reducing all dissolved iron species to Fe(II) with sulfite before analysis. Fe(III) stocks were prepared daily from serial dilutions of 0.0179 mol L⁻¹ certified Fe(III) AA standard (Fisher Scientific) in 0.001 mol L⁻¹ HCl. Total iron standards were prepared in 125-mL Teflon bottles by adding appropriate amounts of secondary stock to 100 mL of out patch surface seawater. All total iron standards received chemical treatment at the same time as the samples to be analyzed.

Total Fe samples and standards were acidified to pH 2.0 for 12 h using Optima HCl. After this short-term acidification, all samples and standards were buffered to pH 4.8 (efficient for Fe(III) reduction by sulfite [Millero et al. 1995a]) with acetate buffer. We found it was important to add only the minimal amount of buffer needed to achieve pH 4.8, as excess buffering capacity interfered with the luminol reaction and resulted in inaccurate total Fe determinations. Sodium sulfite then was added to a final concentration of 200 μmol L⁻¹ and reacted for 12 h at room temperature.

Standard additions were analyzed in triplicate on a seawater sample to give the slope for the standard curve. This analytical approach was preferable to preparation of standards in deionized water because it took into account any possible matrix effects on the luminol reaction chemistry, and it prevented salinity-derived mixing differences in the flow cell. The total Fe standard curve was linear across the range analyzed (0–1.5 nmol L⁻¹ total Fe added). The individual slopes of the total Fe regression lines varied more than that of the Fe(II) analyses. We found that these fluctuations were not because of differences in the natural seawater matrix, but probably were due to very small differences in buffering capacity among sample runs (data not shown). The reagent blank was determined as 40 pmol L⁻¹ by performing standard

additions on the buffer and sulfite in MilliQ water. A subset of Fe(III) determinations using this reductive method were compared to values obtained using the Obata chemiluminescent Fe(III) method (1993).

Fe(II) oxidation rates—The plumbing of the FeLume system was adapted to determine picomolar Fe(II) oxidation rates for a range of temperatures (4.0–21.0°C) by bypassing the injection valve, thereby enabling a continuous stream of sample and luminol reagent to mix in the plexiglas reaction coil. Plumbed in this way, the system provided uninterrupted measurement of changing Fe(II) levels with time. Samples were placed in a temperature-controlled bath (Neslab), and all pH measurements used the free ion scale with Tris buffers and an Accumet AP62 electrode calibrated according to Millero (1986). The pH of the seawater used in these experiments was adjusted to 8.00 at 21.0°C using dilute ammonia or HCl and calculated at the other temperatures according to Millero (1995). Once adjusted to the appropriate temperature, the samples were saturated with O₂ by bubbling with air that had been passed through a KMnO₄ solution to prevent H₂O₂ contamination from laboratory air.

Seawater samples for Fe(II) oxidation studies were stored in the dark for 24 h to enable complete decay of ambient Fe(II) and other radicals that would contribute to Fe(II) oxidation (Eqs. 1–4). A number of unfiltered samples were collected in parallel for comparison of Fe(II) oxidation rates in unfiltered water. The samples were spiked with Fe(II) to an initial concentration of 100 pmol L⁻¹ and were pumped directly to the reaction spiral while the PMT signal was continuously recorded. The change in Fe(II) signal was recorded over 10 min for each sample and was performed in triplicate for each temperature. Periodic fluctuations in PMT signal (from pump noise and periodic fluctuations in the ship's power) were removed from the decay curves. Between replicates, the reaction spiral was rinsed with 0.1 mol L⁻¹ HCl to remove mineral precipitates that form at high pH. The attenuation of chemiluminescence signal from these precipitates was insignificant as compared to the signal decay from Fe(II) oxidation (data not shown).

Picomolar Fe(II) oxidation experiments were repeated in ultraviolet (UV)-treated seawater collected cleanly from Ocean Station PAPA in June 2006. The seawater was irradiated by suspending a mercury pen lamp (UVP) into an acid-cleaned quartz tube and submerging the quartz tube into a reflective 1-liter Teflon bottle for 48 h. After a 48-h irradiation period, the seawater was stored in the dark for 9 months, enabling the removal of any photochemically generated reactive oxygen species. The samples were then adjusted to pH 8.00 at 21.0°C, brought to the appropriate temperature, and saturated with air (*see above*) before conducting the oxidation experiments.

Results

Vertical profiles of Fe(II)—Vertical profiles of Fe(II) were measured on two independent casts in HNLC surface waters outside of the iron-fertilized patch (Fig. 2A,B). Both profiles were collected just after mid-day (~12:00–13:30 h

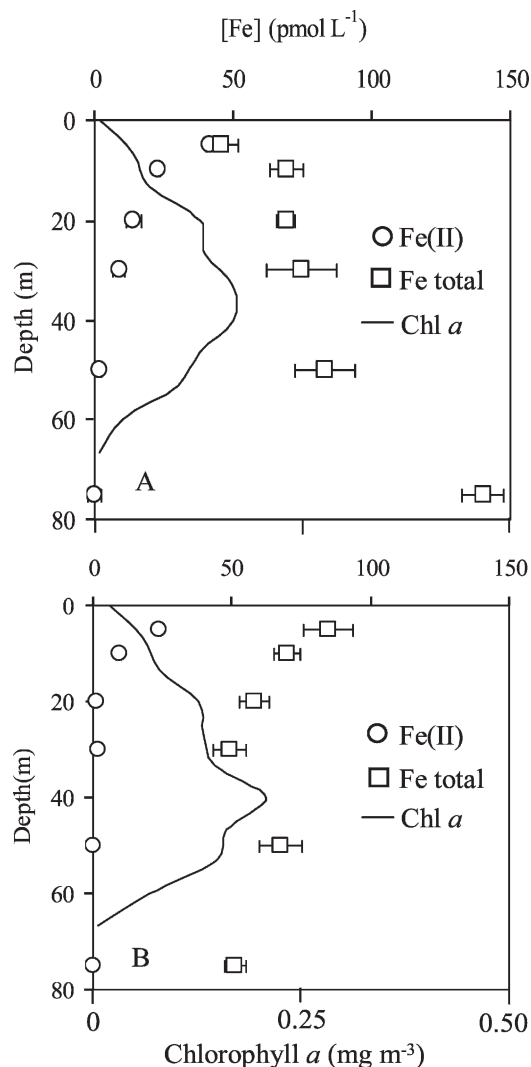


Fig. 2. Vertical profiles of Fe(II) and total Fe from two out-patch stations. (A) Profile on 14 Aug 2004 at 12:30 h local time under a sunny sky. (B) Profile sampled on 04 Aug 2004 at 13:00 h local time under an overcast sky. Open circles represent analytical Fe(II) concentrations, and open squares represent total Fe concentrations in the samples. The solid line represents the relative chlorophyll *a* concentration, as determined by *in vivo* fluorescence. Data points are the mean of triplicate analyses whereas error bars represent ± 1 SD. The 5-m total Fe datum in panel A is considered suspect because it was inconsistent with independent measurements (*see text*).

local time). Each profile shows the highest Fe(II) concentrations at the surface and values decreasing with depth to undetectable levels below 50 m. Surface Fe(II) concentrations were markedly higher on 14 Aug 2004, 40 pmol L⁻¹ Fe(II), than the previous profile on 04 Aug 2004, 25 pmol L⁻¹ Fe(II). Although no luminosity data are available for these days, the profile on 14 Aug 2004 (Fig. 2A) was obtained under a clear sunny sky, whereas the profile on 04 Aug 2004 (Fig. 2B) was collected under an overcast sky. The vertical profiles of Fe(II) did not correlate with phytoplankton biomass in either cast, indicated here by the chlorophyll *a* fluorescence trace in Fig. 2A,B.

Vertical profiles of total dissolved iron—Total dissolved ($0.2 \mu\text{m}$) iron concentrations were determined at the same depths as the Fe(II) measurements, and these data are plotted in relation to Fe(II) in Fig. 2A,B. Unlike the consistent patterns observed in the vertical profiles of Fe(II), there were significant differences in total Fe between the two sampling dates. A surface minimum of 45 pmol L^{-1} total Fe was observed on 14 Aug, with a maximum of 140 pmol L^{-1} total Fe at $\sim 75 \text{ m}$. In contrast, the surface maximum was 80 pmol L^{-1} total Fe on 04 Aug, which decreased to 50 pmol L^{-1} at 75 m . A comparison on board between the FeLume method and the Obata chemiluminescence technique (Obata et al. 1993), operated by the Institute of Ocean Sciences group (Sydney, Canada), on the 14 Aug profile showed generally consistent results, with the exception of the unusually low total Fe value at 5-m depth. The differences between the total iron profiles collected roughly 1 week apart likely reflects the complex and changing water masses observed along the immediate periphery of the fertilized patch during the SEEDS II experiment.

Transect of Fe(II) and total iron in surface waters—To better understand the relationship between Fe(II) and total dissolved iron in surface waters, concentrations of both were measured in a surface transect crossing the SEEDS II iron-fertilized patch 7 days after the second iron infusion (Fig. 3A,B). There was a sharp gradient in Fe(II) concentration on both sides of the enriched patch, changing from $\sim 25 \text{ pmol L}^{-1}$ in unfertilized water to $>200 \text{ pmol L}^{-1}$ inside the patch. Fe(II) oxidation measurements (see below) show that the elevated Fe(II) in the patch could not have been a residual signal from the Fe(II) infusion 7 d earlier, but instead must have resulted from in situ reductive processes.

Fe(II) oxidation rates—The temperature dependence of Fe(II) oxidation was measured in both UV oxidized (ligand-free) and ambient HNLC surface seawater ($\text{pH} = 8.00$ at 21°C) between 4.0°C and 21.0°C using 100 pmol L^{-1} Fe(II) additions. Napierian log transformation of Fe(II) chemiluminescence over time showed linear decreases in signal at all temperatures, indicating pseudo-first-order kinetics for Fe(II) oxidation during the timescale monitored. The Fe(II) oxidation rate constant, k_{ox} (min^{-1}), determined as the slope of log-transformed chemiluminescence signal, increased with temperature (Fig. 4). Values of k_{ox} (min^{-1}) for natural surface and UV-treated waters were corrected for temperature effect on K_w , temperature effect on carbonate system pK_a (Millero 1995), and adjusted to equivalent Fe(II) oxidation rates at $\text{pH} 8.00$ (Santana-Casiano et al. 2005), assuming saturated oxygen concentrations (Garcia and Gordon 1992). The corrected Fe(II) oxidation rates were fitted to the equation

$$\log k_{\text{ox}} = 15.65 - 5005/T \quad (5)$$

for a temperature range of 4.0 – 21.0°C for 24-h dark aged natural surface seawater and

$$\log k_{\text{ox}} = 18.5 - 5725/T \quad (6)$$

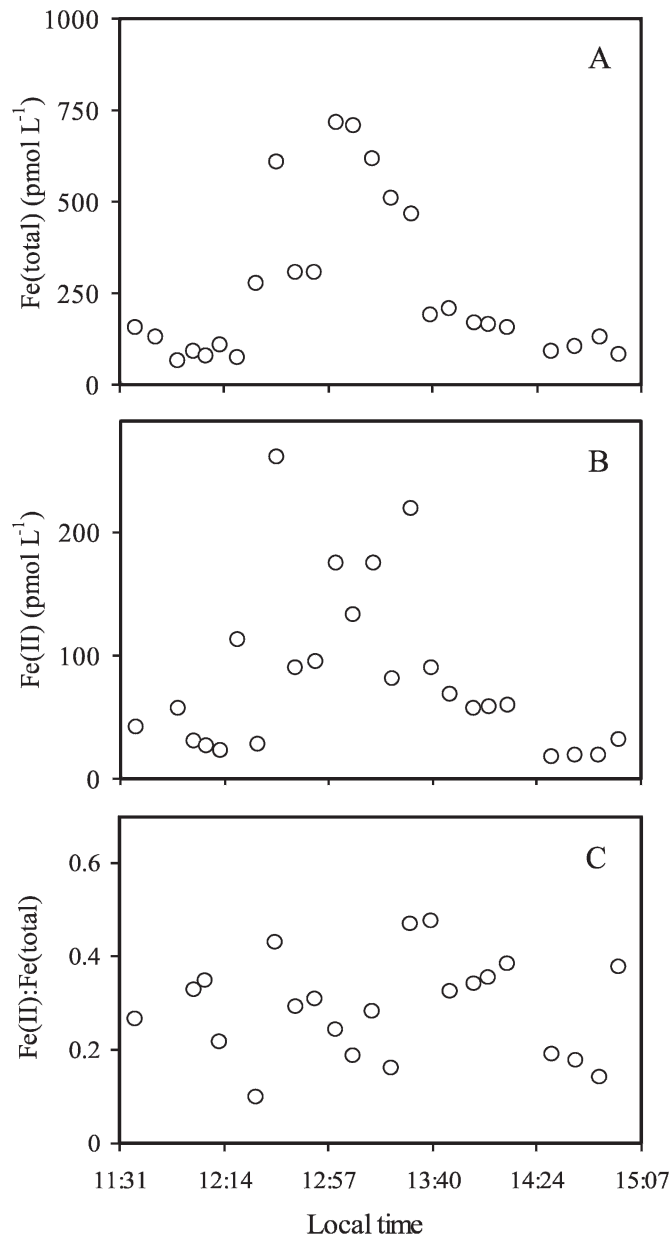


Fig. 3. Spatial distribution of (A) total Fe, (B) Fe(II), and (C) the ratio of Fe(II):total Fe along a transect crossing the core of the SEEDS II fertilized patch. Data points are the mean of triplicate analyses.

for the same temperature range for UV-treated seawater (Fig. 4). These relationships yield activation energies (42 kJ mol^{-1} and 47.5 kJ mol^{-1} , respectively) comparable to nanomolar Fe(II) oxidation experiments measured in Gulf Stream seawater (45 kJ mol^{-1} [Santana-Casiano et al. 2005]). A summary of results from this work is given in Fig. 5 and Table 1. UV oxidation had a marked effect on Fe(II) half-life, with values at a 4.0 , 10.0 , 18.0 and 21.0°C being \sim two-fold higher in natural surface water.

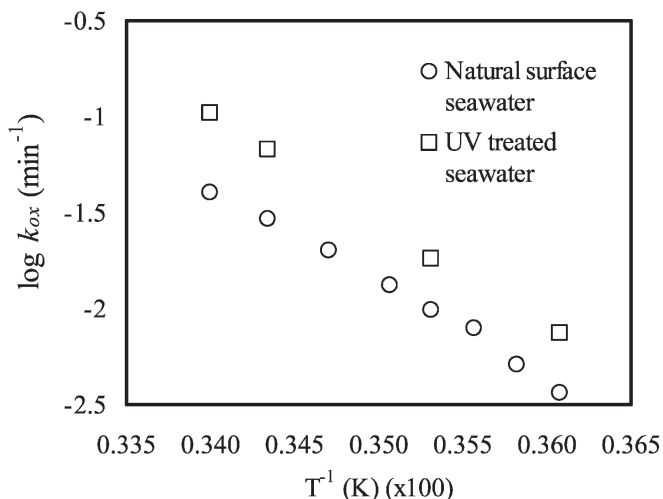


Fig. 4. Experimentally determined pseudo-first-order rate constants k_{ox} (min^{-1}) for Fe(II) oxidation in ambient HNLC subarctic Pacific surface waters (open circles), and UV-treated seawater (open squares) as a function of reciprocal temperature (K^{-1}). All rates were corrected to pH 8.00 (see text), and linear fits to these data are given by Eqs. 5 and 6 in the text.

Discussion

Studies of iron chemistry in seawater during the last decade or more have demonstrated that the chemical speciation of Fe(III) is dominated by complexation with functionally metal-specific organic ligands (see Rue and Bruland 1997), and Fe(II) species largely have been presumed to at best have a trace and ephemeral presence. The findings here challenge that assumption by showing that Fe(II) can comprise a significant proportion of total dissolved iron in subarctic Pacific surface waters at midday.

There are three potential direct sources of Fe(II) in oxic surface waters: wet deposition (Faust and Zepp 1993), photochemical production in situ (Wells et al. 1991; Johnson et al. 1994), and biological reduction induced by either electron shuttles (Kustka et al. 2005; Rose et al. 2005) or cell surface reductases (Maldonado and Price 2001). Iron is one of the more abundant trace metals in rain, and its redox transformations affect the chemistry of atmospheric waters (Faust and Zepp 1993). A major fraction of this iron is maintained in Fe(II) species (see Kieber et al. 2001) by either continual photoproduction or from stabilization by organic ligands (Kieber et al. 2005). However, there were no significant rain events during the sampling period here, and no relationship was found between salinity and Fe(II) concentrations (data not shown), indicating that wet deposition was not the source of Fe(II) in these surface waters. There also was no correlation between the vertical profiles of Fe(II) and chlorophyll fluorescence, which suggests that Fe(II) was not produced biologically. Moreover, Fe(II) concentrations dropped below detectable levels in nighttime surface samples as well as over short-term (24 h) storage of unfiltered seawater in the dark (Table 2). Although these independent observations do not preclude cell surface Fe(III) reduction having a significant role in iron uptake

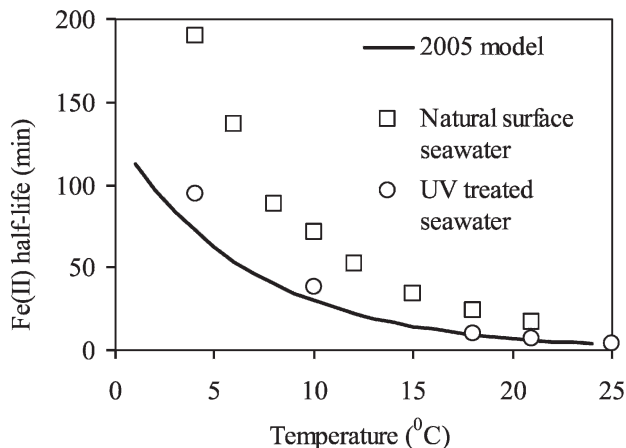


Fig. 5. Fe(II) half-lives as a function of temperature. Half-lives for natural surface waters (open squares) and UV-treated seawater (open circles) are calculated using experimentally determined pseudo-first-order rate constants, and the rates in UV-treated and natural surface waters were corrected to equivalent rates pH 8.00 (see text). Model data (solid line) are from González-Davila et al. (2005).

(Shaked et al. 2005; Maldonado et al. 2006; Salmon et al. 2006), this process apparently had little effect on the oxidation state of iron in the bulk seawater.

The exponential decrease in Fe(II) concentrations with depth, measured under full sunlight (14 Aug), is consistent with in situ photochemical reduction being the primary source of Fe(II). Photochemical reduction of Fe(III) in colloids (Wells et al. 1991; Kuma et al. 1992) by direct ligand-to-metal-charge transfer in Fe(III)-organic complexes (Kuma et al. 1992; Barbeau et al. 2001) and indirectly by biologically or photochemically produced superoxide (Rose et al. 2005; Voelker and Sedlak 1995; Fujii et al. 2006) has been demonstrated in marine waters, so this linkage is not surprising. However, the degree that photolysis influences the overall redox state of iron in these HNLC surface waters is unexpected, with upwards of 50% of the dissolved iron pool existing as Fe(II) species during midday. It is unclear whether the photolysis is direct or indirect via the generation of O_2^- and H_2O_2 by photolysis of dissolved organic matter.

The photochemical effects on iron redox chemistry were found in both ambient and fertilized surface (5 m) waters, with Fe(II) comprising a major fraction of total dissolved iron throughout the transect (Fig. 3C). Total dissolved iron concentrations increased from $\sim 70 \text{ pmol L}^{-1}$ outside the patch to $\sim 700 \text{ pmol L}^{-1}$ in the patch core, and Fe(II) concentrations also changed by an order of magnitude ($\sim 20 \text{ pmol L}^{-1}$ to $\sim 200 \text{ pmol L}^{-1}$). These changes occurred in parallel so that the ratio of Fe(II):total Fe remained relatively constant (Fig. 3C), suggesting perhaps that some steady-state kinetic reactions were taking place. This possibility cannot be properly assessed here because the relevant reactive oxygen species (Eqs. 2–4) were not measured. However, the apparent coupling between Fe(II) and total iron suggests that Fe(II) production rates were approximately first-order with respect to total iron concentration. This finding is consistent with a photochem-

Table 1. Measured and corrected Fe(II) oxidation rates for natural and ultraviolet (UV)-treated seawater.

T (°C)	Measured rates				Corrected rates*		
	24-hour dark aged surface water		UV-treated surface water		24-hour dark aged surface water	UV-treated surface water	Model prediction†
	log k_{ox} (min ⁻¹)	±	log k_{ox} (min ⁻¹)	±	log k_{ox} (min ⁻¹)	log k_{ox} (min ⁻¹)	log $k_{predicted}$ (min ⁻¹)
4	-2.03	0.09	-1.73	0.12	-2.44	-2.13	-2.02
6	-1.95	0.07			-2.30		-1.89
8	-1.81	0.08			-2.11		-1.76
10	-1.76	0.09	-1.50	0.09	-2.01	-1.74	-1.64
12	-1.68	0.06			-1.88		-1.51
15	-1.57	0.07			-1.70		-1.32
18	-1.47	0.08	-1.11	0.08	-1.53	-1.18	-1.13
21	-1.39	0.04	-0.98	0.03	-1.39	-0.94	-0.95

* Corrected for temperature dependence of pK_w and carbonate system pK_a (Millero 1995). Rates were then adjusted to equivalent rates at pH 8.00 according to Santana-Casiano et al. (2005).

† Calculated from second-order rate constants at pH 8.00 (Santana-Casiano et al. 2005), multiplied by saturated oxygen concentrations at given temperature (Garcia and Gordon 1992).

ical source of Fe(II) if all dissolved Fe(III) was photochemically active. It is important to note that the elevated Fe(II) concentrations measured in the patch occurred more than a week after the mesoscale Fe(II) enrichment; sufficient time for the infused Fe(II) to fully oxidize, according to our rate measurements.

To our knowledge, this study is the first to measure Fe(II) oxidation rates in natural seawater at near-ambient (<100 pmol L⁻¹) Fe(II) concentrations. This capability enables us to investigate the potential for subnanomolar organic ligand concentrations to affect Fe(II) oxidation rates in natural seawater. Indeed, these experiments yielded an unexpected result. The pseudo-first-order Fe(II) oxidation rate constants in ambient surface water at 21.0°C were 61% (±8) slower than rates measured in ligand-free seawater, and similar slower rates were observed across a range of temperatures (Fig. 5). Here, we compare rate constants at 21.0°C because pH was measured accurately (±0.01) at this temperature, rather than calculated at other temperatures, and we therefore can better quantify and propagate error due to uncertainty in pH measurements.

The measured Fe(II) oxidation rates in natural surface water are significantly slower than measured in UV-treated seawater, as well as that predicted from inorganic processes (Santana-Casiano et al. 2005) (Fig. 5), although we are uncertain whether error propagation in these model results complicate this comparison.

There are at least two possible explanations to account for slower Fe(II) oxidation rates in these waters: decreased concentrations of reactive oxygen species involved in Fe(II) oxidation (Eqs. 2, 3, and 4), or pseudo-stabilization of Fe(II) by organic complexation. The scavenging of reactive oxygen species is known to affect Fe(II) oxidation rates at nanomolar Fe(II) concentrations (*see* Rose and Waite 2003), but would not be significant in our subnanomolar Fe(II) experiments. Seawater used in our oxidation experiments was filtered (to remove potential cellular sources of reactive oxygen species) and aged a minimum of 24 hours in the dark, so initial concentrations of superoxide and hydroxyl radicals would be negligible. Although hydrogen peroxide was not measured here, our measurements in similar waters show that concentrations (<60 nmol L⁻¹)

Table 2. Fe(II) concentrations in samples collected during day, night, and after 24-h dark aging.

Sample name	Collection date	Unfiltered samples				
		Collection time (local)	[Fe(II)] (pmol L ⁻¹)	± (1 SD)		
In patch 5 m	27 Jul 2004	14:00	214	6		
	28 Jul 2004	03:25	1	4		
Out patch 5 m	04 Aug 2004	13:00	23	1		
	05 Aug 2004	02:00	0	2		
Out patch 5 m	14 Aug 2004	12:30	41	2		
	14 Aug 2004	23:00	0	2		
Unfiltered samples collected and dark aged for 24 hours						
Sample name	Collection date	Collection time (local)	Initial [Fe(II)] (pmol L ⁻¹)	± (1 SD)	Final [Fe(II)] (pmol L ⁻¹)	± (1 SD)
Out patch 5 m	01 Aug 2004	15:40	19	2	0	2
Out patch 5 m	02 Aug 2004	12:15	29	4	0	3

would not be high enough to affect Fe(II) oxidation rates (Santana-Casiano et al. 2006). Taking into account the low levels of Fe(II) added (100 pmol L⁻¹) and the short duration of oxidation experiments (10 min), the maximum superoxide concentration that could be generated by the end of the experiment (Eq. 1) was ≤ 50 pmol L⁻¹. Even assuming a fast second-order rate constant for Fe(II) oxidation by superoxide (10⁷ L mol⁻¹ s⁻¹), superoxide-associated oxidation would account for <1% of the observed rate. It is unlikely then that free radicals generated during our oxidation experiments significantly affected Fe(II) oxidation rates.

There has been no direct measurement to date of Fe(II) complexation by organic ligands in natural seawater, however, the observation that Fe(II) oxidation rates were faster in UV-treated seawater (after aging of the seawater to eliminate reactive oxygen species) strongly suggests that organic ligands exerted some influence on Fe(II) speciation in these HNLC waters. We now explore this possibility in more detail.

The overall oxidation rate of inorganic iron is a function of its chemical speciation [Fe²⁺, FeOH⁺, Fe(OH)₂⁰, Fe(CO₃), Fe(CO₃)₂²⁻] and their respective oxidation rate constants (Millero 1989; King 1998; Santana-Casiano et al. 2005) The distribution coefficient of each inorganic Fe(II) species in seawater is well described.

$$\alpha_i = \frac{K'_i[i]}{(1 + \sum_i K'_i[i])} \quad (7)$$

where $[i]$ is the analytical ligand concentration of each inorganic ligand, and (K'_i) is the conditional stability constant for each species. Thus the effective Fe(II) oxidation rate is the sum of the product of each Fe(II) distribution coefficient (α_i) and its second-order oxidation rate constant (k_i) for oxidation by oxygen.

$$\frac{d\text{Fe(II)}}{dt} = -[\text{Fe(II)}][\text{O}_2] \sum_i \alpha_i k_i \quad (8)$$

Thermodynamic ion-pairing models predict that the fraction of hydrated Fe²⁺ $\alpha_{\text{Fe}^{2+}}$ is 0.76 at pH 8.00 (Millero et al. 1995b). However, this species oxidizes very slowly, and Fe(II) oxidation is controlled instead by trace Fe(II) species [Fe(OH)₂⁰, Fe(CO₃)₂²⁻] that oxidize much faster.

The distribution coefficient and oxidation rate expressions can be modified to include the effects from Fe(II) complexing organic ligand species

$$\alpha'_i = \frac{K_i[i]}{\left(1 + \left(\sum_i K'_i[i]\right) + ([\text{Org}]K_{\text{org}})\right)} \quad (9)$$

$$\frac{d\text{Fe(II)}}{dt} = -[\text{Fe(II)}][\text{O}_2] \left(\sum_i \alpha_i k_i + \alpha_{\text{org}} k_{\text{org}}\right) \quad (10)$$

where $[\text{Org}]$ and K_{org} are the concentration and mean conditional stability constant of a given class of Fe(II) complexing organic ligands believed to be in the sample. In principle, the formation of Fe(II)–organic complexes can either accelerate or decelerate Fe(II) oxidation in seawater

depending on their structure (Rose and Waite 2003). Our findings suggest that Fe(II)–organic complexes in these HNLC waters are less reactive to oxidation and indeed were a significant fraction of the total Fe(II) species.

Assuming the purported Fe(II)–organic complexes were nonreactive to oxidation by oxygen, our observed reduction in Fe(II) oxidation rates at 21.0°C indicates a 61% (± 8) decrease in concentrations of Fe²⁺ and the associated kinetically reactive inorganic Fe(II) species. (The fraction of Fe²⁺ ($\alpha_{\text{Fe}^{2+}}$) is the reciprocal of denominator in Eqs. 7 and 9.) Without additional knowledge of organic ligand concentration or conditional constant, we can calculate only the product of $[\text{Org}]$ and K_{org} in Eq. 9. Based on the known inorganic speciation of Fe(II), this product must then be on the order of two. If we assume that the concentrations of Fe(II) complexing ligands are on the same order as Fe(III) complexing ligands in seawater (~ 10 – 100 nmol L⁻¹), the corresponding aggregate conditional constant (K_{org}) ranges from 10⁸ to 10⁹. If we assume the forward rate constant for Fe(II) complexation is equivalent to the rate of water loss for Fe(II) ($\sim 4 \times 10^6$ s⁻¹ [Crumbliss and Garrison 1988]), the metal-ligand dissociation rate would be on the order of 10⁻³ s⁻¹ or faster. At these rates, the aggregate of Fe(II) complexes would dissociate quickly enough that $\alpha_{\text{Fe}^{2+}}$ would remain relatively constant throughout our oxidation experiments, and only the inorganic Fe(II) species would be oxidized. In this case, Fe(II) complexing ligands could serve only to slow Fe(II) oxidation, rather than completely stabilizing Fe(II) in seawater. This outcome is consistent with our observations that samples stored in the dark for 24 h or samples collected at night had no measurable Fe(II) (Table 2). This also could explain the similarity among the activation energies of Fe(II) oxidation in western subarctic Pacific surface water, UV-treated seawater, and Gulf Stream seawater (Santana-Casiano et al. 2005) because the temperature dependence of inorganic Fe(II) oxidation by O₂ lies mostly in the temperature effect on K_w . It is worth noting that many of the previous studies of Fe(II) oxidation kinetics would not have captured the effect of organic ligands because free ligand concentrations would have been greatly exceeded by the relatively high (>100 nmol L⁻¹) Fe(II) concentrations used.

In contrast, strong Fe(II) complexing organic ligands have been reported in rainwater (Kieber et al. 2005), and these ligands continue to stabilize Fe(II) for hours, even when mixed with oligotrophic seawater (Kieber et al. 2005). Clearly, the ligand effects in the HNLC surface waters studied here are different. We can speculate that the type of ligand responsible for stabilizing Fe(II) would have relatively “soft” functional groups (e.g., amine, thiol). Not only can the thermodynamic formation constants for these types of Fe(II)–Org complexes range between 10⁸–10³⁰ (Martel and Smith 1982), but phytoplankton have been shown to produce ligands having thiol functional groups in response to elevated copper concentrations (see Dupont et al. 2004). We speculate further that the Fe(II) complexation inferred by our measurements and calculations may represent one of the side reactions of the strong copper complexing ligands measured in the subarctic

Pacific (Coale and Bruland 1988) and also shown to be released by *Synechococcus* spp. (Moffett and Brand 1995); a picoplanktonic group present in subarctic Pacific waters.

Iron fluxes to surface waters of the western subarctic Pacific from advective upwelling and aerosol deposition normally are insufficient to fuel large diatom blooms, as demonstrated by two mesoscale iron enrichment experiments (Tsuda et al. 2003; Tsuda et al. pers. comm.). But diatoms and other nanoplankton clearly are unable to fully utilize ambient iron present in these HNLC waters because dissolved iron concentrations (~ 100 pmol L⁻¹) lie well above diffusion-limited thresholds for diatom growth (Hudson and Morel 1993; Sunda and Huntsman 1995; Wells 2003). In the Fé model for iron acquisition by phytoplankton (Hudson and Morel 1993), uptake is proportional to the concentration of free inorganic iron (Fe³⁺), which in seawater is lowered to sub-picomolar levels by strong Fe(III)-specific organic ligands (see Rue and Bruland 1997). However, more recent models suggest that Fe(II) species may be more important for regulating iron uptake (Shaked et al. 2005; Salmon et al. 2006), suggesting that photochemical processes should directly increase iron availability. But even though Fe(II) species indeed comprised a major fraction of total dissolved iron in SEEDS II surface waters, this Fe(II) was not readily available to diatoms and other eukaryotic phytoplankton. Alternatively, if oxidation of Fe(II) at the cell membrane surface by copper activated enzymes is required for transport, as implied in one high-affinity iron uptake model for some diatoms (Maldonado and Price 2001; Wells et al. 2005), then copper co-limitation could also restrict Fe(II) acquisition. Indeed very low-level copper (nmol L⁻¹) amendments to these HNLC waters increased eukaryotic growth (Trick et al. pers. comm.). Alternatively, Fe(II)-organic complexes proposed here to explain the slower observed iron oxidation may render Fe(II) more inaccessible to cellular uptake centers. In any event, the findings here indicate that iron availability to diatoms is not alleviated even by a dynamic iron redox cycle that maintains a major fraction of dissolved iron as Fe(II) in western subarctic Pacific surface waters.

References

- BARBEAU, K., E. L. RUE, K. W. BRULAND, AND A. BUTLER. 2001. Photochemical cycling of iron in the surface ocean mediated by microbial iron(III)-binding ligands. *Nature* **413**: 409–413.
- BRAND, L. E., W. G. SUNDA, AND R. R. L. GUILLARD. 1983. Limitation of marine phytoplankton reproductive rates by zinc, manganese, and iron. *Limnol. Oceanogr.* **28**: 1182–1198.
- COALE, K. H., AND K. W. BRULAND. 1988. Copper complexation in the Northeast Pacific. *Limnol. Oceanogr.* **33**: 1084–1101.
- CROOT, P. L., AND OTHERS. 2001. Retention of dissolved iron and Fe(II) in an iron induced Southern Ocean phytoplankton bloom. *Geophys. Res. Lett.* **28**: 3425–3428.
- CRUMBLISS, A. L., AND J. M. GARRISON. 1988. A comparison of some aspects of the aqueous coordination chemistry of aluminum (III) and iron (III). *Comments Mod. Chem.* **8**: 1–26.
- DUPONT, C. L., R. K. NELSON, S. BASHIR, J. W. MOFFETT, AND B. A. AHNER. 2004. Novel copper-binding and nitrogen-rich thiols produced and exuded by *Emiliania huxleyi*. *Limnol. Oceanogr.* **49**: 1754–1762.
- FAUST, B. C., AND R. G. ZEPP. 1993. Photochemistry of aqueous iron(III)-polycarboxylate complexes: Roles in the chemistry of atmospheric and surface waters. *Environ. Sci. Tech.* **27**: 2517–2522.
- FUJII, M., A. L. ROSE, T. D. WAITE, AND T. OMURA. 2006. Superoxide-mediated dissolution of amorphous ferric oxyhydroxide in seawater. *Environ. Sci. Tech.* **40**: 880–887.
- GARCIA, H. E., AND L. I. GORDON. 1992. Oxygen solubility in seawater: Better fitting equations. *Limnol. Oceanogr.* **37**: 1307–1312.
- HUDSON, R. J. M., AND F. M. M. MOREL. 1993. Trace metal transport by marine microorganisms: implications of metal coordination kinetics. *Deep-Sea Res. Oceanogr. Res. Paper.* **40**: 129–150.
- JOHNSON, K. S., K. H. COALE, V. A. ELROD, AND N. W. TINDALE. 1994. Iron photochemistry in seawater from the equatorial Pacific. *Mar. Chem.* **46**: 319–334.
- KIEBER, R. J., S. A. SKRABAL, B. J. SMITH, AND J. D. WILLEY. 2005. Organic complexation of Fe(II) and its impact on the redox cycling of iron in rain. *Environ. Sci. Tech.* **39**: 1576–1583.
- , K. WILLIAMS, J. D. WILLEY, S. SKRABAL, AND G. B. AVERY. 2001. Iron speciation in coastal rainwater: Concentration and deposition to seawater. *Mar. Chem.* **73**: 83–95.
- KING, D. W. 1998. Role of carbonate speciation on the oxidation rate of Fe(II) in aquatic systems. *Environ. Sci. Tech.* **32**: 2997–3003.
- , H. A. LOUNSBURY, AND F. J. MILLERO. 1995. Rates and mechanism of Fe(II) oxidation at nanomolar total iron concentrations. *Environ. Sci. Tech.* **29**: 818–824.
- KUMA, K., S. NAKABAYASHI, Y. SUZUKI, I. KUDO, AND K. MATSUNAGA. 1992. Photo-reduction of iron(III) by dissolved organic substances and existence of iron(II) in seawater during spring blooms. *Mar. Chem.* **37**: 15–27.
- KUSTKA, A. B., Y. SHAKED, A. J. MILLIGAN, D. W. KING, AND F. M. M. MOREL. 2005. Extracellular production of superoxide by marine diatoms: Contrasting effects on iron redox chemistry and bioavailability. *Limnol. Oceanogr.* **50**: 1172–1180.
- LAGLERA, L. M., AND C. M. G. VAN DEN BERG. 2007. Wavelength dependence of the photochemical reduction of iron in arctic seawater. *Environ. Sci. Tech.* **41**: 2296–2302.
- MALDONADO, M. T., A. E. ALLEN, J. S. CHONG, K. LIN, D. LEUS, N. KARPENKO, AND S. L. HARRIS. 2006. Copper-dependent iron transport in coastal and oceanic diatoms. *Limnol. Oceanogr.* **51**: 1729–1743.
- , AND N. M. PRICE. 2001. Reduction and transport of organically bound iron by *Thalassiosira oceanica* (Bacillariophyceae). *J. Phycol.* **37**: 298–309.
- MARTEL, A. E., AND R. M. SMITH. 1982. *Critical stability constants*. Plenum Press.
- MILLER, W. L., D. W. KING, J. LIN, AND D. R. KESTER. 1995. Photochemical redox cycling of iron in coastal seawater. *Mar. Chem.* **50**: 63–77.
- MILLERO, F. J. 1986. The pH of estuarine waters. *Limnol. Oceanogr.* **31**: 839–847.
- . 1989. Effect of ionic interactions on the oxidation of iron(II) and copper(I) in natural waters. *Mar. Chem.* **28**: 1–18.
- . 1995. Thermodynamics of the carbon dioxide system in the oceans. *Geochim. Cosmochim. Acta* **59**: 661–677.
- , M. GONZALEZ-DAVILA, AND J. M. SANTANA-CASIANO. 1995a. Reduction of Fe(III) with sulfite in natural waters. *J. Geophys. Res.* **100**: 7235–7244.
- , W. YAO, AND J. AICHER. 1995b. The speciation of Fe(II) and Fe(III) in natural waters. *Mar. Chem.* **50**: 21–39.

- MOFFETT, J. W., AND L. E. BRAND. 1995. Production of strong, extracellular Cu chelators by marine cyanobacteria in response to Cu stress. *Limnol. Oceanogr.* **41**: 388–395.
- O'SULLIVAN, D. W., P. J. NEALE, R. B. COFFIN, T. J. BOYD, AND C. L. OSBURN. 2005. Photochemical production of hydrogen peroxide and methylhydroperoxide in coastal waters. *Mar. Chem.* **97**: 14–33.
- OBATA, H., H. KARATANI, AND E. NAKAYAMA. 1993. Automated determination of iron in seawater by chelating resin concentration and chemiluminescence detection. *Anal. Chem.* **65**: 1524–1528.
- ROSE, A. L., T. P. SALMON, T. LUKONDEH, B. A. NEILAN, AND T. D. WAITE. 2005. Use of superoxide as an electron shuttle for iron acquisition by the marine cyanobacterium *Lyngbya majuscula*. *Environ. Sci. Tech.* **39**: 3708–3715.
- , AND T. D. WAITE. 2002. Kinetic model for Fe(II) oxidation in seawater in the absence and presence of natural organic matter. *Environ. Sci. Tech.* **36**: 433–444.
- , AND ———. 2003. Effect of dissolved natural organic matter on the kinetics of ferrous iron oxygenation in seawater. *Environ. Sci. Tech.* **37**: 4877–4886.
- RUE, E. L., AND K. W. BRULAND. 1997. The role of organic complexation on ambient iron chemistry in the equatorial Pacific Ocean and the response of a mesoscale iron addition experiment. *Limnol. Oceanogr.* **42**: 901–910.
- SALMON, T. P., A. L. ROSE, B. A. NEILAN, AND T. D. WAITE. 2006. The FeL model of iron acquisition: nondissociative reduction of ferric complexes in the marine environment. *Limnol. Oceanogr.* **51**: 1744–1754.
- SANTANA-CASIANO, J. M., M. GONZALEZ-DAVILA, AND F. J. MILLERO. 2006. The role of Fe(II) species on the oxidation of Fe(II) in natural waters in the presence of O₂ and H₂O₂. *Mar. Chem.* **99**: 70–82.
- , ———, AND ———. 2005. Oxidation of nanomolar levels of Fe(II) with oxygen in natural waters. *Environ. Sci. Tech.* **39**: 2073–2079.
- SHAKED, Y., A. B. KUSTKA, AND F. M. M. MOREL. 2005. A general kinetic model for iron acquisition by eukaryotic phytoplankton. *Limnol. Oceanogr.* **50**: 872–882.
- SUNDA, W. G., AND S. A. HUNTSMAN. 1995. Iron uptake and growth limitation in oceanic and coastal phytoplankton. *Mar. Chem.* **50**: 189–206.
- TSUDA, A., et al. 2003. A mesoscale iron enrichment in the western subarctic Pacific induces a large centric diatom bloom. *Science* **300**: 958–961.
- VOELKER, B. M., AND D. L. SEDLAK. 1995. Iron reduction by photo-produced superoxide in seawater. *Mar. Chem.* **50**: 93–102.
- WELLS, M. L. 2003. The level of iron enrichment required to initiate diatom blooms in HNLC waters. *Mar. Chem.* **82**: 101–114.
- , L. M. MAYER, O. F. X. DONARD, M. M. DE SOUZA SIERRA, AND S. G. ACKELSON. 1991. The photolysis of colloidal iron in the oceans. *Nature* **353**: 248–250.
- , AND C. G. TRICK. 2004. Controlling iron availability to phytoplankton in iron-replete coastal waters. *Mar. Chem.* **86**: 1–13.
- , ———, W. P. COCHLAN, M. P. HUGHES, AND V. L. TRAINER. 2005. Domoic acid: The synergy of iron, copper, and the toxicity of diatoms. *Limnol. Oceanogr.* **50**: 1908–1917.
- XIAO, C., D. A. PALMER, D. J. WESOLOWSKI, S. B. LOVITZ, AND D. W. KING. 2002. Carbon dioxide effects on luminol and 1,10-phenanthroline chemiluminescence. *Anal. Chem.* **74**: 2210–2216.

Received: 2 February 2007

Accepted: 28 August 2007

Amended: 10 September 2007